Paper 0123456789

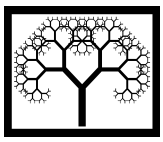

Proceedings of the Fourth International Conference on Parallel, Distributed, Grid and Cloud Computing for Engineering, P. Iványi and B.H.V. Topping (Editors), Civil-Comp Press, Stirlingshire, Scotland.

A New Variant of the Path-Following Algorithm for the Parallel Solving of the Stokes Problem with Friction

M. Jarosova, R. Kucera and V. Satek
IT4Innovations
VSB Technical University of Ostrava
Czech Republic

Abstract

The Stokes problem with the slip boundary condition is approximated using the TFETI domain decomposition method. A new variant of the path-following algorithm for solving the respective algebraic problem is proposed. Numerical experiments illustrate the computational performance.

Keywords: Stokes problem, slip boundary condition, active set algorithm, interior point algorithm, TFETI domain decomposition method.

1 Introduction

In some applications a variable tangential velocity of the fluid along a boundary may depend on a material quality or a shape of the wall. Such behaviour of the fluid is usually simulated by the *slip boundary condition* describing friction between the fluid and the wall; see [1, 2] and references therein. Conditions of this type are used also in contact problems of solid mechanics, where they describe friction laws between bodies [3]. Namely, we consider the slip boundary condition analogous to the Tresca friction law from the solid mechanics.

The contribution deals with the Stokes flow with the slip boundary condition approximated by the TFETI (Total Finite Element Tearing and Interconnecting) domain decomposition method that enables to propose an efficient parallel implementation [4]. To illustrate difficulties and still to keeping the ideas as clear as possible, we consider the planar domain decomposed into several non-overlapping subdomains. The solution continuity on subdomain interfaces is enforced by the Lagrange multipliers. Two other Lagrange multipliers are introduced along the slip boundary to ensure the impermeability of the wall and to regularize the non-differentiable frictional term representing the slip boundary condition. The stability of the mixed finite element approach

together with the stability of the Lagrange multipliers require to use the P1-bubble/P1 finite elements satisfying the *inf-sup* condition [2]. For such elements, the velocity as well as the pressure solution components are approximated by the continues finite element functions so that the solution continuity on the domain interfaces is enforced for both components (velocity and pressure). Computations start from the algebraic dual formulation of the problem that is the minimization of an energy quadratic functional in terms of the Lagrange multipliers constrained by simple bounds and linear equalities. We test two algorithms. The first one is based on an active set strategy (AS) [5]. The second one, that is developed in this work, is a new variant of the path-following (PF) type interior-point method from [6]. Numerical experiments presented in this contribution summarize the performance of the algorithm AS. The result on the algorithm PF will be reported in the oral presentation. Our first experiences with the solution of this problem without the TFETI published in [7] show that the algorithm PF [6] should be more promising.

2 Formulation

Let Ω be a bounded domain in $\mathbb{R}^2$ with a sufficiently smooth boundary $\partial\Omega$ that is split into three disjoint parts: $\partial\Omega = \overline{\gamma}_D \cup \overline{\gamma}_N \cup \overline{\gamma}_C$. We consider the model of a viscous incompressible Newtonian fluid modelled by the Stokes equations with the Dirichlet and Neumann boundary conditions on γ_D and γ_N, respectively, and with the impermeability and the slip boundary conditions prescribed on γ_C:

$$\left.\begin{array}{rcll} -\nu\Delta\mathbf{u} + \nabla \mathtt{p} &=& \mathbf{f} & \text{in } \Omega, \\ \nabla\cdot\mathbf{u} &=& 0 & \text{in } \Omega, \\ \mathbf{u} &=& \mathbf{u}_D & \text{on } \gamma_D, \\ \boldsymbol{\sigma} &=& \boldsymbol{\sigma}_N & \text{on } \gamma_N, \\ \mathtt{u}_n &=& 0 & \text{on } \gamma_C, \\ |\sigma_t| &\le& \mathtt{g} & \text{on } \gamma_C, \\ |\sigma_t(\mathbf{x})| < \mathtt{g}(\mathbf{x}) \;\Rightarrow\; \mathtt{u}_t(\mathbf{x}) &=& 0 & \mathbf{x}\in\gamma_C, \\ |\sigma_t(\mathbf{x})| = \mathtt{g}(\mathbf{x}) \;\Rightarrow\; \exists k := k(\mathbf{x}) \ge 0:\; \mathtt{u}_t(\mathbf{x}) &=& -k\sigma_t(\mathbf{x}) & \mathbf{x}\in\gamma_C, \end{array}\right\} \quad (1)$$

where the shear stress is:

$$\boldsymbol{\sigma} = \nu\frac{\mathrm{d}\mathbf{u}}{\mathrm{d}\mathbf{n}} - \mathtt{p}\mathbf{n}.$$

Here, $\mathbf{u} = (\mathtt{u}_1, \mathtt{u}_2)$ is the flow velocity, $\mathtt{p}$ is the pressure, $\mathbf{f} = (\mathtt{f}_1, \mathtt{f}_2)$ represents forces acting on the fluid, $\nu > 0$ is the kinematic viscosity, and $\mathbf{u}_D$, $\boldsymbol{\sigma}_N$ are given the Dirichlet and Neumann boundary data, respectively. Further $\mathbf{n}$, $\mathbf{t}$ are the unit outer normal and tangential vectors to $\partial\Omega$, respectively, and $\mathtt{u}_n = \mathbf{u}\cdot\mathbf{n}$, $\mathtt{u}_t = \mathbf{u}\cdot\mathbf{t}$ are the normal, tangential components of $\mathbf{u}$ along γ_C, respectively. Finally, $\sigma_t = \boldsymbol{\sigma}\cdot\mathbf{t}$ is the tangential shear stress and $\mathtt{g} \ge 0$ is the slip bound function on γ_C. We will assume that $\gamma_D \neq \emptyset$ and $\gamma_C \neq \emptyset$. For the sake of simplicity we will suppose that $\mathbf{u}_D = \mathbf{0}$.

Next we present the weak velocity-pressure formulation of (1). To this end we

introduce the following notation:

$$V(\Omega) = \{\mathbf{v} \in \left(H^1(\Omega)\right)^2 : \ \mathbf{v} = \mathbf{0} \ \text{ on } \gamma_D, \ \mathtt{v}_n = 0 \ \text{ on } \gamma_C\}$$

and

$$a(\mathbf{v},\mathbf{w}) = \nu \int_\Omega \nabla\mathbf{v} : \nabla\mathbf{w}\, d\mathbf{x}, \quad b(\mathbf{v},\mathtt{q}) = -\int_\Omega \mathtt{q}(\nabla\cdot\mathbf{v})\, d\mathbf{x},$$

$$l(\mathbf{v}) = \int_\Omega \mathbf{f}\cdot\mathbf{v}\, d\mathbf{x} + \int_{\gamma_N} \boldsymbol{\sigma}_N\cdot\mathbf{v}\, ds, \quad j(\mathbf{v}) = \int_{\gamma_C} \mathtt{g}|\mathtt{v}_t|\, ds,$$

where $\nabla\mathbf{v} : \nabla\mathbf{w} = \nabla\mathtt{v}_1\cdot\nabla\mathtt{w}_1 + \nabla\mathtt{v}_2\cdot\nabla\mathtt{w}_2$, $\mathbf{v} = (\mathtt{v}_1,\mathtt{v}_2)$, $\mathbf{w} = (\mathtt{w}_1,\mathtt{w}_2)$.

The velocity-pressure formulation of (1) reads as follows:

$$\left.\begin{array}{l} \textit{Find } (\mathbf{u},\mathtt{p}) \in V(\Omega)\times L^2(\Omega) \textit{ such that} \\ a(\mathbf{u},\mathbf{v}-\mathbf{u}) + b(\mathbf{v}-\mathbf{u},\mathtt{p}) + j(\mathbf{v}) - j(\mathbf{u}) \ge l(\mathbf{v}-\mathbf{u}) \quad \forall \mathbf{v}\in V(\Omega), \\ b(\mathbf{u},\mathtt{q}) = 0 \quad \forall \mathtt{q}\in L^2(\Omega). \end{array}\right\} \tag{2}$$

The following theorem guarantees the existence and uniqueness of a weak solution.

Theorem 1 [2, 8] *Let* $\mathbf{f}\in(L^2(\Omega))^2$, $\boldsymbol{\sigma}_N\in(L^2(\gamma_N))^2$, *and* $\mathtt{g}\in L^\infty(\gamma_C)$, $\mathtt{g}\ge 0$. *Then the first component* $\mathbf{u}$ *of (2) exists and is unique. If* $\gamma_N \neq \emptyset$, *then the pressure* $\mathtt{p}$ *is unique as well, otherwise is unique up to an additive constant.*

An approximation of (2) based on mixed finite elements requires to satisfy the *inf-sup* condition [8]. We use P1-bubble/P1 finite elements as implemented by Koko [8]. It is proved by Ayad, Baffico, Gdoura, and Sassi [2] that this finite element pair is stable also to the Lagrange multipliers realizing the impermeability and the slip boundary conditions. This fact was experimentally verified by Kučera, Haslinger, Šátek, and Jarošová [7]. In order to increase the computational efficiency, we use the TFETI domain decomposition method proposed by Dostál, Horák, and Kučera [4]. To this end, we consider non-overlapping subdomains Ω_r, $1\le r\le s$, so that $\overline{\Omega} = \bigcup_{r=1}^s \overline{\Omega}_r$ and we decompose the problem (2) into Ω_r. The continuity of the solution components approximating $\mathbf{u}$ and $\mathtt{p}$ is enforced by the Lagrange multipliers.

3 Algebraic problems

The TFETI approximation of (2) together with an appropriate quadrature formula approximating the non-differentiable term j leads to the following algebraic problem:

$$\left.\begin{array}{l} \textit{Find } (\mathbf{u},\mathbf{p},\boldsymbol{\lambda}_u,\boldsymbol{\lambda}_p,\boldsymbol{\lambda}_n) \in \mathbb{R}^{2n_p}\times\mathbb{R}^{n_p}\times\mathbb{R}^{2(n_i+n_d)}\times\mathbb{R}^{n_i}\times\mathbb{R}^{n_c} \textit{ such that} \\ \mathbf{u}^\top\mathbf{A}(\mathbf{v}-\mathbf{u}) + (\mathbf{v}-\mathbf{u})^\top\mathbf{B}^\top\mathbf{p} + (\mathbf{v}-\mathbf{u})^\top\mathbf{B}_u^\top\boldsymbol{\lambda}_u + \\ \qquad +(\mathbf{v}-\mathbf{u})^\top\mathbf{N}^\top\boldsymbol{\lambda}_n + \mathbf{g}^\top(|\mathbf{Tv}| - |\mathbf{Tu}|) \ge \mathbf{l}^\top(\mathbf{v}-\mathbf{u}) \quad \forall \mathbf{v}\in\mathbb{R}^{2n_p}, \\ \mathbf{Bu} - \mathbf{Ep} + \mathbf{B}_p^\top\boldsymbol{\lambda}_p = \mathbf{c}, \quad \mathbf{B}_u\mathbf{u} = \mathbf{0}, \quad \mathbf{B}_p\mathbf{p} = \mathbf{0}, \quad \mathbf{Nu} = \mathbf{0}, \end{array}\right\} \tag{3}$$

where $\mathbf{A} = \mathit{diag}(\mathbf{A}_1, \ldots, \mathbf{A}_s) \in \mathbb{R}^{2n_p \times 2n_p}$ is the stiffness matrix with the symmetric, positive semidefinite diagonal blocks, $\mathbf{B} = \mathit{diag}(\mathbf{B}_1, \ldots, \mathbf{B}_s) \in \mathbb{R}^{n_p \times 2n_p}$ represents the divergence operator, $\mathbf{B}_u = (\mathbf{B}_{u,1}, \ldots, \mathbf{B}_{u,s}) \in \mathbb{R}^{2(n_i+n_d) \times 2n_p}$ enforces the velocity continuity and the Dirichlet boundary conditions, $\mathbf{B}_p = (\mathbf{B}_{p,1}, \ldots, \mathbf{B}_{p,s}) \in \mathbb{R}^{n_i \times n_p}$ enforces the pressure continuity, $\mathbf{N} = \mathit{diag}(\mathbf{N}_1, \ldots, \mathbf{N}_s) \in \mathbb{R}^{n_c \times 2n_p}$ and $\mathbf{T} = \mathit{diag}(\mathbf{T}_1, \ldots, \mathbf{T}_s) \in \mathbb{R}^{n_c \times 2n_p}$ collects the normal and tangential vectors to $\partial\Omega$, respectively, at the nodes lying on $\overline{\gamma}_C \backslash \overline{\gamma}_D$, $\mathbf{E} = \mathit{diag}(\mathbf{E}_1, \ldots, \mathbf{E}_s) \in \mathbb{R}^{n_p \times n_p}$ and $\mathbf{c} = (\mathbf{c}_1^\top, \ldots, \mathbf{c}_s^\top)^\top \in \mathbb{R}^{n_p}$ are the stabilization terms arising from the P1-bubble/P1 finite elements (the blocks $\mathbf{E}_r$ are symmetric, positive semidefinite), $\mathbf{l} = (\mathbf{l}_1^\top, \ldots, \mathbf{l}_s^\top)^\top \in \mathbb{R}^{2n_p}$ is given by the forces and the Neumann data, and $\mathbf{g} \in \mathbb{R}_+^{n_c}$ contains the discrete slip bound values. Here, $|\mathbf{x}| = (|x_1|, \ldots, |x_{n_c}|)^\top$ for $\mathbf{x} \in \mathbb{R}^{n_c}$; n_p is the total number of the nodes of triangulations contained in $\overline{\Omega}_r$, $1 \le r \le s$, n_i is the number of the nodes lying on interfaces between subdomains in which the continuity is enforced, n_d is the number of the nodes lying on $\overline{\gamma}_D$, and n_c is the number of the nodes lying on $\overline{\gamma}_C \backslash \overline{\gamma}_D$. Note that the components of $\mathbf{u} = (\mathbf{u}_1^\top, \ldots, \mathbf{u}_s^\top)^\top$ and $\mathbf{p} = (\mathbf{p}_1^\top, \ldots, \mathbf{p}_s^\top)^\top$ correspond to the subdomains Ω_r, $1 \le r \le s$. The blocks $\mathbf{N}_r$, $\mathbf{T}_r$ are zero, if $\overline{\Omega}_r \cap \overline{\gamma}_c = \emptyset$, $1 \le r \le s$.

The unknowns $\boldsymbol{\lambda}_u, \boldsymbol{\lambda}_p, \boldsymbol{\lambda}_n$ play the role of the Lagrange multipliers. Another Lagrange multiplier $\boldsymbol{\lambda}_t \in \mathbb{R}^{n_c}$ will regularize the non-differentiable frictional term in (3) (given by absolute value terms). To this end, we introduce the Lagrangian to (3) $\mathcal{L} : \mathbb{R}^{3n_p} \times \Lambda \mapsto \mathbb{R}$ by

$$\mathcal{L}(\mathbf{y}, \boldsymbol{\mu}) = \frac{1}{2}\mathbf{y}^\top \mathbf{K}\mathbf{y} - \mathbf{y}^\top \mathbf{h} + \boldsymbol{\mu}^\top \mathbf{C}\mathbf{y} \quad (\mathbf{y}, \boldsymbol{\mu}) \in \mathbb{R}^{3n_p} \times \Lambda,$$

with

$$\Lambda = \mathbb{R}^{3n_i+2n_d+n_c} \times \{\boldsymbol{\mu}_t \in \mathbb{R}^{n_c} : \ |\boldsymbol{\mu}_t| \le \mathbf{g}\},$$

where $\mathbf{y} = (\mathbf{y}_1^\top, \ldots, \mathbf{y}_s^\top)^\top$, $\mathbf{y}_r = (\mathbf{v}_r^\top, \mathbf{q}_r^\top)^\top$ couples the velocity and the pressure components, $\boldsymbol{\mu} = (\boldsymbol{\mu}_u^\top, \boldsymbol{\mu}_p^\top, \boldsymbol{\mu}_n^\top, \boldsymbol{\mu}_t^\top)^\top$ collects all Lagrange multipliers, and

$$\mathbf{K} = \mathit{diag}(\mathbf{K}_1, \ldots, \mathbf{K}_s) \in \mathbb{R}^{3n_p \times 3n_p}, \quad \mathbf{K}_r = \begin{pmatrix} \mathbf{A}_r & \mathbf{B}_r^\top \\ \mathbf{B}_r & -\mathbf{E}_r \end{pmatrix},$$

$$\mathbf{h} = (\mathbf{h}_1^\top, \ldots, \mathbf{h}_s^\top)^\top \in \mathbb{R}^{3n_p}, \quad \mathbf{h}_r = \begin{pmatrix} \mathbf{l}_r \\ \mathbf{c}_r \end{pmatrix},$$

$$\mathbf{C} = (\mathbf{C}_1, \ldots \mathbf{C}_s) \in \mathbb{R}^{(3n_i+2n_d+2n_c) \times 3n_p}, \quad \mathbf{C}_r = \begin{pmatrix} \mathbf{B}_{u,r} & \mathbf{0} \\ \mathbf{0} & \mathbf{B}_{p,r} \\ \mathbf{N}_r & \mathbf{0} \\ \mathbf{T}_r & \mathbf{0} \end{pmatrix}.$$

The variational problem (3) is equivalent to the following saddle-point formulation:

$$\textit{Find } (\mathbf{x}, \boldsymbol{\lambda}) \in \mathbb{R}^{3n_p} \times \Lambda \textit{ s.t. } \mathcal{L}(\mathbf{x}, \boldsymbol{\mu}) \le \mathcal{L}(\mathbf{x}, \boldsymbol{\lambda}) \le \mathcal{L}(\mathbf{y}, \boldsymbol{\lambda}) \ \ \forall (\mathbf{y}, \boldsymbol{\mu}) \in \mathbb{R}^{3n_p} \times \Lambda. \quad (4)$$

The velocity and the pressure components can be eliminated by

$$\mathbf{x} = \mathbf{K}^+(\mathbf{h} - \mathbf{C}^\top \boldsymbol{\lambda}) + \mathbf{R}\boldsymbol{\alpha}, \quad (5)$$

where $\mathbf{K}^+$ is a generalized inverse to $\mathbf{K}$ satisfying $\mathbf{K} = \mathbf{K}\mathbf{K}^+\mathbf{K}$, $\mathbf{R}$ is the matrix whose columns are a basis of the null-space of $\mathbf{K}$, and $\boldsymbol{\alpha} \in \mathbb{R}^{2s}$ is a new unknown. Obviously, $\mathbf{R} = diag(\mathbf{R}_1, \ldots, \mathbf{R}_s) \in \mathbb{R}^{3n_p \times 2s}$ and

$$\mathbf{R}_r = \begin{pmatrix} \mathbf{1} & \mathbf{0} \\ \mathbf{0} & \mathbf{1} \\ \mathbf{0} & \mathbf{0} \end{pmatrix},$$

where $\mathbf{1}$ and $\mathbf{0}$ are the vectors of all ones and all zeros, respectively. Substituting (5) into the first inequality in (4), we arrive at the dual problem in terms of $\boldsymbol{\lambda}$:

$$\textit{Find } \boldsymbol{\lambda} \in \Lambda^{\#} \textit{ such that } \mathcal{S}(\boldsymbol{\lambda}) \leq \mathcal{S}(\boldsymbol{\mu}) \quad \forall \boldsymbol{\mu} \in \Lambda^{\#}, \tag{6}$$

where

$$\Lambda^{\#} = \{\boldsymbol{\mu} \in \Lambda : \ \mathbf{G}\boldsymbol{\mu} = \mathbf{e}\} \quad \text{and} \quad \mathcal{S}(\boldsymbol{\mu}) = \frac{1}{2}\boldsymbol{\mu}^\top \mathbf{F}\boldsymbol{\mu} - \boldsymbol{\mu}^\top \mathbf{d}$$

with $\mathbf{G} = \mathbf{R}^\top \mathbf{C}^\top$, $\mathbf{e} = \mathbf{R}^\top \mathbf{h}$, $\mathbf{F} = \mathbf{C}\mathbf{K}^+\mathbf{C}^\top$, and $\mathbf{d} = \mathbf{C}\mathbf{K}^+\mathbf{h}$. Note the $\mathbf{F}$ is non-singular on the null-space of $\mathbf{G}$. After computing $\boldsymbol{\lambda}$ from (6), one can obtain $\boldsymbol{\alpha}$ using

$$\boldsymbol{\alpha} = -(\mathbf{R}^\top \mathbf{C}_{\mathcal{I}}^\top \mathbf{C}_{\mathcal{I}} \mathbf{R})^{-1} \mathbf{R}^\top \mathbf{C}_{\mathcal{I}}^\top \mathbf{C}_{\mathcal{I}} \mathbf{K}^+ (\mathbf{h} - \mathbf{C}^\top \boldsymbol{\lambda}),$$

where $\mathbf{C}_{\mathcal{I}}$ is defined by the matrix $\mathbf{T}_{\mathcal{I}}$ instead of $\mathbf{T}$ and it arises from $\mathbf{T}$ by omitting its rows corresponding to the index set $\mathcal{I} = \{i : \ |\lambda_{t,i}| < g_i, \ 1 \leq i \leq n_c\}$.

4 Path-following algorithm

In this section, we introduce main ideas of the path-following variant of the interior point algorithm developed from [6].

Let the Lagrangian to (6) be defined by

$$L(\boldsymbol{\lambda}, \boldsymbol{\nu}) = \mathcal{S}(\boldsymbol{\lambda}) + \boldsymbol{\mu}_1^\top(-\boldsymbol{\lambda}_t - \mathbf{g}) + \boldsymbol{\mu}_2^\top(\boldsymbol{\lambda}_t - \mathbf{g}) + \boldsymbol{\mu}_3^\top \mathbf{G}(\boldsymbol{\lambda} - \mathbf{e}),$$

where $\boldsymbol{\nu} = (\boldsymbol{\mu}_1^\top, \boldsymbol{\mu}_2^\top, \boldsymbol{\mu}_3^\top)^\top \in \mathbb{R}^{2n_c+2s}$ is the Lagrange multiplier associated with the two-side constraint and the equality constraint appearing in $\Lambda^{\#}$. Let $\boldsymbol{\mu} = (\boldsymbol{\mu}_1^\top, \boldsymbol{\mu}_2^\top)^\top$ and let $\mathbf{z} := -\nabla_\mu L(\boldsymbol{\lambda}, \boldsymbol{\nu})$ be the new variable. We introduce the function

$$\mathbf{H} : \mathbb{R}^{3n_i+2n_d+6n_c+2s} \mapsto \mathbb{R}^{3n_i+2n_d+6n_c+2s},$$

$$\mathbf{H}(\mathbf{w}) := (\nabla_\lambda L(\boldsymbol{\lambda}, \boldsymbol{\nu})^\top, (\nabla_\mu L(\boldsymbol{\lambda}, \boldsymbol{\nu}) + \mathbf{z})^\top, \mathbf{1}^\top \mathbf{M}\mathbf{Z}, \nabla_{\mu_3} L(\boldsymbol{\lambda}, \boldsymbol{\nu})^\top)^\top,$$

where $\mathbf{w} = (\boldsymbol{\lambda}^\top, \boldsymbol{\mu}^\top, \mathbf{z}^\top, \boldsymbol{\mu}_3^\top)^\top \in \mathbb{R}^{3n_i+2n_d+6n_c+2s}$, $\mathbf{M} = diag(\boldsymbol{\mu})$, $\mathbf{Z} = diag(\mathbf{z})$, and $\mathbf{1} \in \mathbb{R}^{2n_c}$ is the vector of all ones. The solution $\bar{\boldsymbol{\lambda}}$ to (6) is the first component of the vector $\bar{\mathbf{w}} = (\bar{\boldsymbol{\lambda}}^\top, \bar{\boldsymbol{\mu}}^\top, \bar{\mathbf{z}}^\top, \bar{\boldsymbol{\mu}}_3^\top)^\top$, which satisfies

$$\mathbf{H}(\mathbf{w}) = \mathbf{0}, \ \boldsymbol{\mu} \geq \mathbf{0}, \ \mathbf{z} \geq \mathbf{0}, \tag{7}$$

since (7) is equivalent to the Karush-Khun-Tucker conditions to the problem (6).

To derive the path-following algorithm, we replace (7) by the following perturbed problem:

$$\mathbf{H}(\mathbf{w}) = (\mathbf{0}^\top, \mathbf{0}^\top, \tau\mathbf{1}^\top, \mathbf{0}^\top)^\top,\ \boldsymbol{\mu} \geq \mathbf{0},\ \mathbf{z} \geq \mathbf{0}, \tag{8}$$

where $\tau \in \mathbb{R}_+$. Solutions $\mathbf{w}^\tau$ to (8) define a curve $\mathcal{C}(\tau)$ in $\mathbb{R}^{3n_i+2n_d+6n_c+2s}$ called the *central path*. This curve approaches $\bar{\mathbf{w}}$ when τ tends to zero. We combine the damped Newton method used for solving the equation in (8) with an appropriate change of τ which guarantees that the iterations belong to a neighbourhood $\mathcal{N}(c_1, c_2)$ of $\mathcal{C}(\tau)$ defined by

$$\begin{aligned}\mathcal{N}(c_1, c_2) \ = \ \{&\mathbf{w} = (\boldsymbol{\lambda}^\top, \boldsymbol{\mu}^\top, \mathbf{z}^\top, \boldsymbol{\mu}_3^\top)^\top \in \mathbb{R}^{3n_i+2n_d+6n_c+2s}\ : \\ &\mu_i z_i \geq c_1\vartheta,\ i = 1, \ldots, 2n_c, \\ &\boldsymbol{\mu} \geq \mathbf{0},\ \mathbf{z} \geq \mathbf{0},\ \|\nabla_\lambda L(\boldsymbol{\lambda}, \boldsymbol{\nu})\| \leq c_2\vartheta,\ \|\nabla_\mu L(\boldsymbol{\lambda}, \boldsymbol{\nu}) + \mathbf{z}\| \leq c_2\vartheta\},\end{aligned} \tag{9}$$

where $c_1 \in (0, 1]$, $c_2 \geq 0$, and $\vartheta := \vartheta(\mathbf{w}) = \boldsymbol{\mu}^\top\mathbf{z}/(2n_c)$. In the k-th iteration, we modify $\tau := \tau^{(k)}$ by the product of $\vartheta^{(k)} = \vartheta(\mathbf{w}^{(k)})$ with the centering parameter $c^{(k)}$ chosen as in [6]. The algorithm uses also the *Armijo-type condition* (11) ensuring that the sequence $\{\vartheta^{(k)}\}$ is monotonically decreasing. By $\mathbf{J}(\mathbf{w})$ in (10), we denote the Jacobi matrix of $\mathbf{H}$ at $\mathbf{w}$.

ALGORITHM PF: Given $c_1 \in (0, 1]$, $c_2 \geq 1$, $0 < c_{\min} \leq c_{\max} \leq 1/2$, $\omega \in (0, 1)$, and $\varepsilon \geq 0$. Let $\mathbf{w}^{(0)} \in \mathcal{N}(c_1, c_2)$ and set $k := 0$.

(i). Choose $c^{(k)} \in [c_{\min}, c_{\max}]$;

(ii). Solve

$$\mathbf{J}(\mathbf{w}^{(k)})\Delta\mathbf{w}^{(k+1)} = -\mathbf{H}(\mathbf{w}^{(k)}) + (\mathbf{0}^\top, \mathbf{0}^\top, c^{(k)}\vartheta^{(k)}\mathbf{1}^\top, \mathbf{0}^\top)^\top; \tag{10}$$

(iii). Set $\mathbf{w}^{(k+1)} = \mathbf{w}^{(k)} + \alpha^{(k)}\Delta\mathbf{w}^{(k+1)}$ with the largest $\alpha^{(k)} \in (0, 1]$ satisfying $\mathbf{w}^{(k+1)} \in \mathcal{N}(c_1, c_2)$ and

$$\vartheta^{(k+1)} \leq (1 - \alpha^{(k)}\omega(1 - c^{(k)}))\vartheta^{(k)}; \tag{11}$$

(iv). Return $\bar{\mathbf{w}} = \mathbf{w}^{(k+1)}$, if $err^{(k)} := \|\mathbf{w}^{(k+1)} - \mathbf{w}^{(k)}\|/\|\mathbf{w}^{(k+1)}\| \leq \varepsilon$, else set $k := k + 1$ and go to step (i).

The bounds on the parameters mentioned in the initialization section follow from the convergence analysis presented in [6]. The computational efficiency depends on a way how the inner linear systems (10) are solved. The Jacobi matrix is non-symmetric, indefinite with the following block structure:

$$\mathbf{J}(\mathbf{w}^{(k)}) = \begin{pmatrix} \mathbf{F} & \mathbf{J}_{12} & \mathbf{0} & \mathbf{G}^\top \\ \mathbf{J}_{12}^\top & \mathbf{0} & \mathbf{I} & \mathbf{0} \\ \mathbf{0} & \mathbf{Z} & \mathbf{M} & \mathbf{0} \\ \mathbf{G} & \mathbf{0} & \mathbf{0} & \mathbf{0} \end{pmatrix}, \quad \mathbf{J}_{12} = \begin{pmatrix} \mathbf{0} & \mathbf{0} \\ -\mathbf{I} & \mathbf{I} \end{pmatrix}.$$

Eliminating the 2nd and 3rd unknown of $\Delta\mathbf{w}^{(k+1)}$, we get the reduced linear system for $\Delta\boldsymbol{\lambda}^{(k+1)}$ and $\Delta\boldsymbol{\mu}_3^{(k+1)}$ with the Schur complement matrix

$$\mathbf{J}_{SC} = \begin{pmatrix} \mathbf{F} + \mathbf{M}_1\mathbf{Z}_1^{-1} + \mathbf{M}_2\mathbf{Z}_2^{-1} & \mathbf{G}^\top \\ \mathbf{G} & \mathbf{0} \end{pmatrix}, \tag{12}$$

where $\mathbf{Z} = diag(\mathbf{Z}_1, \mathbf{Z}_2)$ and $\mathbf{M} = diag(\mathbf{M}_1, \mathbf{M}_2)$. The reduced system can be solved by the *precoditioned projected* conjugate gradient method [4]. In order to guarantee the convergence, we use the preconditioner:

$$\mathbf{P}_{SC} = \begin{pmatrix} \mathbf{D} + \mathbf{M}_1\mathbf{Z}_1^{-1} + \mathbf{M}_2\mathbf{Z}_2^{-1} & \mathbf{G}^\top \\ \mathbf{G} & \mathbf{0} \end{pmatrix},$$

where $\mathbf{D} = diag(\mathbf{F})$. The projector on the null-space of $\mathbf{G}$ reads as follows:

$$\mathbf{P} = \mathbf{I} - \mathbf{G}^\top(\mathbf{G}\mathbf{G}^\top)^{-1}\mathbf{G}$$

As $\boldsymbol{\mu}^{(k)} > \mathbf{0}$, $\mathbf{z}^{(k)} > \mathbf{0}$, the precoditioned and projected operator is symmetric, positive definite on the null-space of $\mathbf{G}$ and its eigenvalues belong to an interval which does not depend on the iteration. Consequently, the spectral condition number is bounded by a constant independent on the iteration (see [6]). In computations, we approximate $\mathbf{D}$ so that $\mathbf{K}^+$ in $\mathbf{F}$ is replaced by $diag(\mathbf{K})^{-1}$.

The conjugate gradient iterations used in the k-th step of ALGORITHM PF are initialized and terminated adaptively. The initial vector is taken as the computed result in the previous (outer) iteration and the (inner) iterations are terminated, if the relative residuum is less than the stopping tolerance given by

$$tol^{(k)} = \min\{r_{tol} \times err^{(k-1)}, c_{fact} \times tol^{(k-1)}\},$$

where $0 < r_{tol} < 1$, $0 < c_{fact} < 1$, $err^{(-1)} = 1$, and $tol^{(-1)} = r_{tol}/c_{fact}$.

5 Numerical experiments

The problem (1) is approximated by the P1-bubble/P1 finite elements on triangular meshes [9]. The frictional term $j(\mathbf{v}_h)$ in (2) is evaluated using the numerical integration:

$$j(\mathbf{v}_h) = \int_{\gamma_C} \mathrm{g}|\mathrm{v}_{ht}|\, ds \approx \sum_{\mathbf{x}_i \in N_{cont}} \omega_i \mathrm{g}(\mathbf{x}_i)|\mathrm{v}_{ht}(\mathbf{x}_i)| =: \mathbf{g}^\top|\mathbf{T}\mathbf{v}|, \tag{13}$$

where N_{cont} is the set of integration points and ω_i are weights of a quadrature formula. Below we use N_{cont} given by triangle vertices (nodes) lying on $\overline{\gamma}_C \backslash \overline{\gamma}_D$. In general, γ_C is approximated by a polygon and ω_i are chosen so that (13) represents the trapezoidal rule over this polygon.

All codes are implemented in Matlab 2013b. The computations were performed by ANSELM supercomputer at IT4I VŠB-TU Ostrava. We use ALGORITHM AS

(called SMALBE in [5]) with $\varepsilon = tol_{AS} \times \|\mathbf{d}\|$, $\Gamma = 1$, $\alpha = 1.9\|\mathbf{F}\|$. The values of these parameters seem to be optimal, as follows from the results in [10, 5, 11]. The terminating tolerances is denoted by tol_{AS}. In tables below we introduce complexities of computations in terms of matrix-vector multiplications by the dual Hessian $\mathbf{F}$ for different numbers of subdomains (s), primal unknowns ($3n_p$), and dual unknowns ($3n_i + 2n_d + 2n_c$). We denote by h and H the norm (diameter) of the finite element triangles and the subdomains, respectively.

Example 1 (square domain with curved slip boundary). Let $\Omega = (0,1) \times (0,1)$, $\gamma_D = (0,1) \times \{1\}$, $\gamma_{N_{left}} = \{0\} \times (0,1)$, $\gamma_{N_{right}} = \{1\} \times (0,1)$, $\gamma_N = \gamma_{N_{left}} \cup \gamma_{N_{right}}$, and $\gamma_C = \{(x, 0.8(x - x^2)) : x \in (0,1)\}$. The data of problem (1) are defined as follows: $\mathbf{f} = -\nu\Delta\mathbf{u}_{exp} + \nabla \mathrm{p}_{exp}$, $\nu = 1$, $\mathbf{u}_D = \mathbf{0}$, $\boldsymbol{\sigma}_N = \boldsymbol{\sigma}_{exp|_{\gamma_N}}$, and $\mathrm{g} = 10$, where $\mathbf{u}_{exp}(x,y) = (-\cos(2\pi x)\sin(2\pi y) + \sin(2\pi y), \sin(2\pi x)\cos(2\pi y) - \sin(2\pi x))$ and $\mathrm{p}_{exp}(x,y) = 2\pi(\cos(2\pi y) - \cos(2\pi x))$. Note that $\mathbf{u}_{exp}$ and p_{exp} do not solve (1). The finite element mesh, the velocity, and the pressure field are drawn in Figure 1.

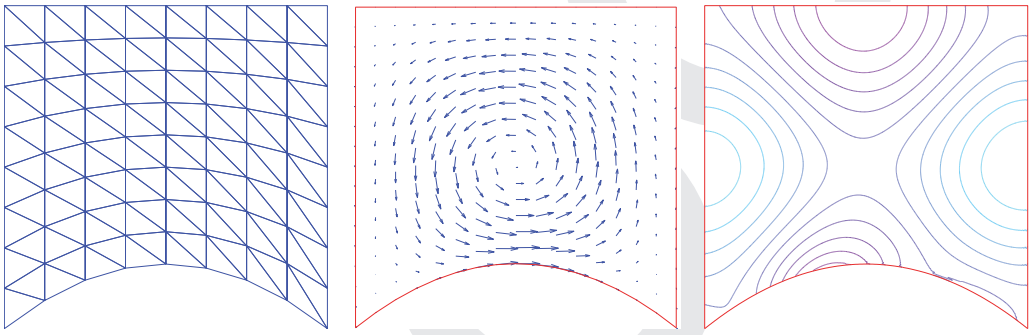

Figure 1: *(Example 1; slip solution,* $\mathrm{g} = 10$*)* Mesh (left), velocity field (middle), isobars (right).

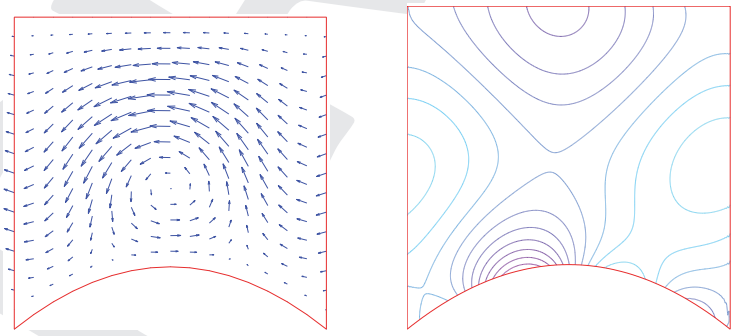

Figure 2: *(Example 1; no-slip solution,* $\mathrm{g} = 40$*)* Velocity field (left), isobars (right).

On γ_C we prescribe different values of g in order to illustrate friction effects that are seen in Figure 3 for slip boundary. The solution for no-slip boundary is shown in Figure 2. In Table 1 and 2 we show the number of matrix-vector multiplications by $\mathbf{F}$

for changing number of subdomains (constant $H/h = 8$) and changing H/h (constant 4×4 number of subdomains), respectively. All results are calculated by $tol_{AS} = 10^{-6}$.

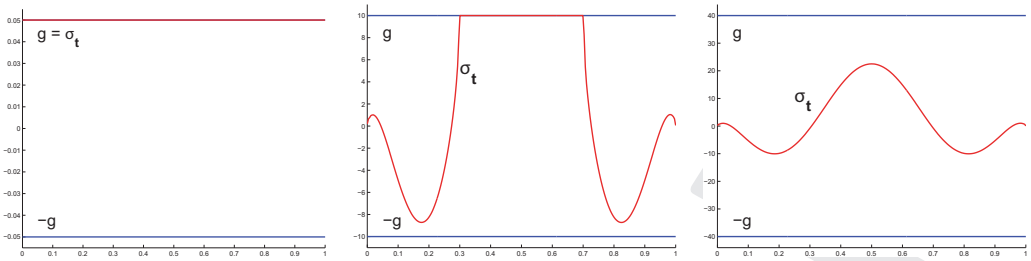

Figure 3: g $= 0.05$ (left), g $= 10$ (middle), g $= 40$ (right).

	slip bound	g $= 0.05$	g $= 10$	g $= 40$
s	primar/dual	AS	AS	AS
4 (2×2)	972/173	**613**	**995**	**259**
16 (4×4)	3888/753	**1528**	**1054**	**1674**
36 (6×6)	8748/1741	**2046**	**2248**	**717**
64 (8×8)	15552/3137	**3399**	**2323**	**1585**
100 (10×10)	24300/4941	**4506**	**6237**	**862**

Table 1: Multiplications by $\mathbf{F}$ for changing number of subdomains and $H/h = 8$.

	slip bound	g $= 0.05$	g $= 10$	g $= 40$
H/h	primar/dual	AS	AS	AS
2	432/225	**909**	**1232**	**1256**
4	1200/401	**1098**	**750**	**578**
8	3888/753	**1466**	**1134**	**3155**
16	13872/1457	**2387**	**13360**	**2939**

Table 2: Multiplications by $\mathbf{F}$ for 4×4 subdomains ($s = 16$) and changing H/h.

Example 2 (channel flow). Let $\Omega = (0, 0.1) \times (0, 0.1)$ The decomposition of the boundary $\partial\Omega$ is as follows: $\gamma_D = \{0\} \times (0, 0.1)$, $\gamma_N = \{0.1\} \times (0, 0.1)$, and $\gamma_C = \gamma_{C,1} \cup \gamma_{C,2}$, $\gamma_{C,1} = (0, 0.1) \times \{0.1\}$, $\gamma_{C,2} = (0, 0.1) \times \{0\}$. The problem (1) is solved for $\mathbf{f} = \mathbf{0}$, $\nu = 1$, $\mathbf{u}_{D|\gamma_D} = (0.1y - y^2, -0.1y + y^2)$ with $y \in (0, 0.1)$, and $\boldsymbol{\sigma}_N = \mathbf{0}$.

In Figure 5 we illustrate friction effects, where the upper, lower graph represents the situation on $\gamma_{C,1}$, $\gamma_{C,2}$, respectively. The solution with g $= 0.015$ is shown in Figure 4. This solution is slipping on γ_C (Figure 5, left). The alternative solution with g $= 0.15$ is partially slipping and partially sticking on $\gamma_{C,2}$ (Figure 5, middle) and the last solution with g $= 10$ is solely sticking on γ_C (Figure 5, right). In Tables 3 and 4

we show the number of matrix-vector multiplications by $\mathbf{F}$ for changing number of subdomains (constant $H/h = 8$) and for changing H/h (constant 4×4 number of subdomains), respectively. All results are calculated by $tol_{AS} = 10^{-3}$.

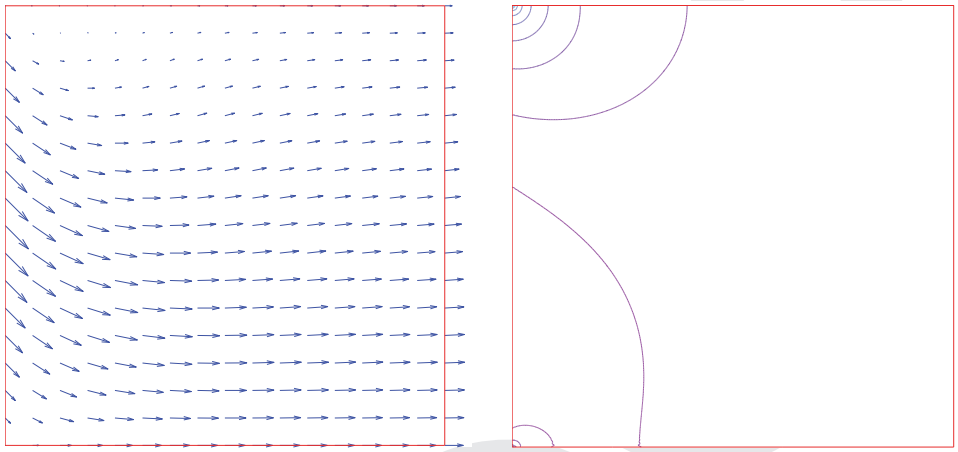

Figure 4: Velocity field (left), isobars (right).

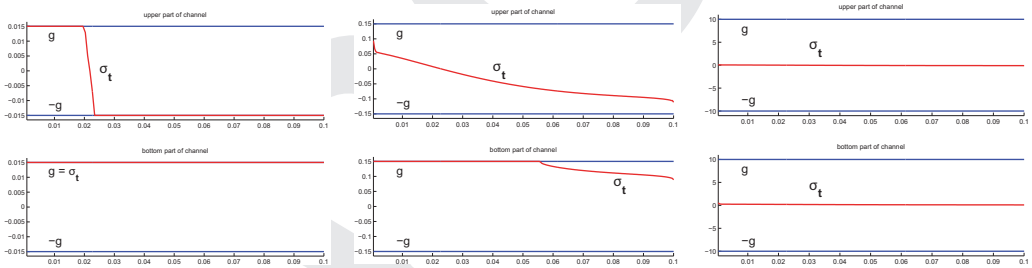

Figure 5: g $= 0.015$ (left), g $= 0.15$ (middle), g $= 10$ (right).

Acknowledgments

This work was supported by the European Development Fund in the IT4Innovations Centre of Excellence (CZ.1.05/1.1.00/02.0070) and by the project New creative teams in priorities of scientific research (CZ.1.07/2.3.00/30.0055) supported by Operational Programme Education for Competitiveness and co-financed by the European Social Fund and the state budget of the Czech Republic. MJ was partially supported by the Grant Agency of the Czech Republic (GACR 13-30657P).

	slip bound	$\mathrm{g} = 0.015$	$\mathrm{g} = 0.15$	$\mathrm{g} = 10$
s	primar/dual	AS	AS	AS
$4(2 \times 2)$	972/173	**1928**	**1626**	**331**
$9(3 \times 3)$	2187/412	**9674**	**1167**	**568**
$16(4 \times 4)$	3888/753	**9826**	**1570**	**709**
$25(5 \times 5)$	6075/1196	**10605**	**1700**	**748**
$36(6 \times 6)$	8748/1741	**25522**	**2289**	**783**
$49(7 \times 7)$	11907/2388	**38566**	**2854**	**833**
$64(8 \times 8)$	15552/3137	**48986**	**3258**	**845**
$81(9 \times 9)$	19683/3988	**65784**	**3953**	**822**
$100(10 \times 10)$	24300/4941	**75915**	**4104**	**1014**

Table 3: Multiplications by $\mathbf{F}$ for changing number of subdomains and $H/h = 8$.

	slip bound	$\mathrm{g} = 0.015$	$\mathrm{g} = 0.15$	$\mathrm{g} = 10$
H/h	primar/dual	AS	AS	AS
2	432/225	**3132**	**1021**	**473**
4	1200/401	**5713**	**1096**	**611**
8	3888/753	**10761**	**1587**	**706**
16	13872/1457	**69171**	**2092**	**820**

Table 4: Multiplications by $\mathbf{F}$ for 4×4 subdomains ($s = 16$) and changing H/h.

References

[1] I. J. Rao, K. R. Rajagopal, The effect of the slip boundary condition on the flow of fluids in a channel, Acta Mechanica, Vol. 135, pp. 113-126, 1999.

[2] M. Ayadi, L. Baffico, M. K. Gdoura, T. Sassi, Error estimates for Stokes problem with Tresca friction conditions, ESAIM: Mathematical Modelling and Numerical Analysis, (accepted 2014).

[3] J. Haslinger, I. Hlaváček, J. Nečas, Numerical methods for unilateral problems in solid mechanics, Analysis, Volume IV, Part 2, North Holland, Amsterdam, 1996.

[4] Z. Dostál, D. Horák, R. Kučera, Total FETI - an easier implementable variant of the FETI method for numerical solution of elliptic PDE, Communications in Numerical Methods in Engineering, Vol. 22:12, pp. 1155-1162, 2006.

[5] Z. Dostál, Optimal quadratic programming algorithms: with applications to variational inequalities, SOIA 23, Springer US, New York, 2009.

[6] R. Kučera, J. Machalová, H. Netuka, P. Ženčák, An interior point algorithm for the minimization arising from 3D contact problems with friction, Optimization Methods and Software, Vol. 28:6, pp. 1195-1217, 2013.

[7] R. Kučera, J. Haslinger, V. Šátek, M. Jarošová, Efficient methods for solving the Stokes problem with slip boundary conditions, submitted to Mathematics and

Computers in Simulation, 2014.
[8] H. C. Elman, D. J. Silvester, A. J. Wathen, Finite Elements and Fast Iterative Solvers with Applications in Incompressible Fluid Dynamics, Oxford University Press, Oxford, 2005.
[9] J. Koko, Vectorized Matlab codes for the Stokes problem with P1-bubble/P1 finite element, at: http://www.isima.fr/∼jkoko/Codes.html, 2012.
[10] Dostál Z., Schöberl J., Minimizing quadratic functions subject to bound constraints with the rate of convergence and finite termination, Comput. Optim. Appl. 30, 2005, pp. 23-44.
[11] Kučera R., Convergence rate of an optimization algorithm for minimizing quadratic functions with separable convex constraints, SIAM Journal on Optimization 19 (2), 2008, pp. 846-862.